REVIEW

Check for updates

Surface modification of liquid metal as an effective approach for deformable electronics and energy devices

Hyunwoo Bark [ID] and Pooi See Lee [ID] *

The fields of flexible or stretchable electronics and energy devices, reconfigurable and compliant soft robotics, wearable e-textiles or health-care devices have paid significant attention to the need of deformable conductive electrodes due to its critical role in device performances. Gallium-based liquid metals, such as the eutectic gallium–indium (EGaIn) being an electrically conductive liquid phase at room temperature, have attracted immense interests as a promising candidate for deformable conductor. However, in the case of bulk liquid metal, there are several limitations such as the need of encapsulation, dispersion in a polymer matrix, or accurate patterning. For these reasons, the preparation of liquid metal particles in harnessing the properties in a non-bulk form and surface modification is crucial for the success of incorporating liquid metal into functional devices. Herein, we discuss the current progress in chemical surface modification and interfacial manipulations of liquid metal particles. The physical and chemical properties of the surface modification-assisted liquid metal polymer composite are also reviewed. Lastly, the applications of the surface-modified liquid metal particles such as flexible electrode, soft robotics, energy storage or harvester, thermal conductor, dielectric sensor, and bioelectronics are discussed, and the corresponding perspectives of deformable electronics and energy devices are provided. In particular, we focus on the functionalization method or requirement of liquid metal particles in each application. The challenging issues and outlook on the applications of surface-modified liquid metal particles are also discussed.

1. Introduction

Developing wearable and flexible electronic materials and devices, which have sustainable electrical properties under mechanical deformation, are gaining immense attention. Generally, the deformable electronic materials are prepared by polymer composite with electrically or thermally conductive fillers such as carbon nanotubes, graphene, or inorganic nanowires.[1–5] However, the performance of the composite is dependent on the percolation of fillers; in other words, the performance of the deformable device could be deteriorated as a function of the mechanical enforcement in materials, such as strain.[6,7] Gallium-based liquid metal is a promising material for flexible and soft electronics because the liquid metal has a liquid phase at room temperature, and is infinitely deformable without sacrificing the electrical performance.[8] With physical properties, liquid metal has shown promising electrical performances for flexible electronics due to its low resistivity (eutectic GaIn: $\sim 29.4 \times 10^{-6}$ Ω-cm).[9] For example, by embedding liquid metal into a patterned fluidic channel area molded with a flexible polymer such as polydimethylsiloxane

(PDMS), the potential of a deformable or soft electronic device has been revealed.[10–12] However, due to the formation of an oxide layer on the bulk liquid metal,[13] the difficulty of precise patterning and wettability on the substrate are challenges encountered in utilizing liquid metal for further processability. For this reason, the liquid metal particles under 10^1 µm have been utilized to overcome these issues. In order to utilize the liquid metal particles, the surface modification on the liquid metal particle surface is necessary. Recently, several strategies for the size control or control dispersion in the polymer matrix have been suggested based on the surface modification of liquid metal particles by controlling the oxide layer formation, chemical compound functionalization, or galvanic replacement.[11,14–19] For example, since the oxide layer on the liquid metal surface grows immediately when the liquid metal is exposed in ambient condition,[20] the formation of the oxide layer determines the shape of the liquid metal. In this case, removing the oxide layer *via* acid treatment or applying an electric field transformed the shape of the liquid metal.[20,21] Moreover, the immediate generation of the oxide on liquid metal provides a way to obtain 10^0 to 10^2 µm scale of liquid metal particles.[22] Using microfluidics, ultrasonication, or shear-mixing, the initial bulk state of the oxide layer is broken, and the new oxide layer can be generated with a smaller size[23–26] (Fig. 1(a)). On the

School of Material Science and Engineering, Nanyang Technological University, 50 Nanyang Avenue, Singapore 639798. E-mail: pslee@ntu.edu.sg

other hand, liquid metal particles can be obtained by chemical functionalization. For instance, thiol group-containing chemical compounds (such as 1-dodecanethiol) drives the formation of a self-assembly monolayer on the liquid metal surface under ultrasonication.[16,27] In addition, carboxyl group-containing molecules are helpful in obtaining liquid metal particles due to the coordination between the carboxyl group and oxide layer.[28–32] Galvanic replacement is another route to the surface functionalization of liquid metal. In metal ion-containing aqueous solution, the surface of the liquid metal particles can be formed by MGa (M = Pt, Ag, Au).[17–19] These surface-modified liquid metal particles have shown potentials in various applications. As introduced above, owing to the outstanding electrical performance, infinite deformation of the liquid metal, ease of dispersion in the polymer matrix, the utilization of the liquid metal has been increasingly widespread in soft electronic devices requiring flexible and stretchable electrodes or thermal conductive channels, energy storage or harvesting, and sensing.[24,25,28,33–39] Besides, the metal (semiconductor)-decorated liquid metal can be utilized as soft robotics. The metal or semiconductor, which is decorated on the liquid metal, plays a significant role of the actuation. In addition, the actuation can be triggered by electric field,[40] catalytic reactions,[41,42] and magnetic field.[43–46] Furthermore, since the metal (semiconductor)-decorated liquid metal is non-wettable on Si, SiO_2, or Teflon, whereas the as-dropped liquid metal with an oxide layer on the liquid metal has adhesion with Si, SiO_2, or Teflon,[46,47] the metal (semiconductor)-decorated liquid metal can be readily manipulated owing to the low rolling friction.[47] Due to the low hazards of the gallium-based liquid metal on human health,[48] there is a potential for a biomedical soft robot.[49]

Herein, we present a review of the surface modification of liquid metal and its use in electronic, soft robotics, electrochemical energy storage, energy harvesters, thermal conductivity, dielectric sensing, and biomaterial applications. We first elucidate the recent progress in the preparation of liquid metal particles exploiting the surface modification by oxide layer formation, chemical compound assisted formation and Galvanic replacement formation (Fig. 1(b)). These surface-modified liquid metal particles can be stable and dispersed in an organic solvent or polymer matrix. Thus, the surface-modified liquid metal particles can be readily fabricated as a liquid metal/polymer composite, core–shell structure, or colloidal suspension, depending on the targeted applications. Herein, we are highlighting the requirements of the surface modification of liquid metal in different applications. We expect this review provides the basic consideration and perspectives on the surface modification of liquid metal for the optimization of their functional properties.

2. Types of liquid metal

Generally, liquid metal is known as a single element or alloy composition with a low melting point, and has a liquid phase at room temperature. The most representative liquid metal is mercury (Hg), which has 234 K of melting point. Hg has been employed in electronic and medical industries. For example, due to the liquid phase of Hg, Hg can be deformed into various shapes, and the electrical conductivity of Hg is 10 400 S m^{-1}.[50] Thus, Hg has been an attractive electrode material, such as the dropping mercury electrode or the mercury film electrode.[51,52] In addition, Hg was used for one of the dental amalgam filling materials.[53] However, due to its high toxicity, the use of Hg is strictly limited. Gallium (Ga)-based liquid metal is regarded as an alternative. Generally, the melting point of Ga is about 303 K, and the electrical resistivity of Ga is $\sim 2.6 \times 10^{-5}$ Ω-cm at room temperature.[54] Due to the similar characteristics of Ga with Hg,
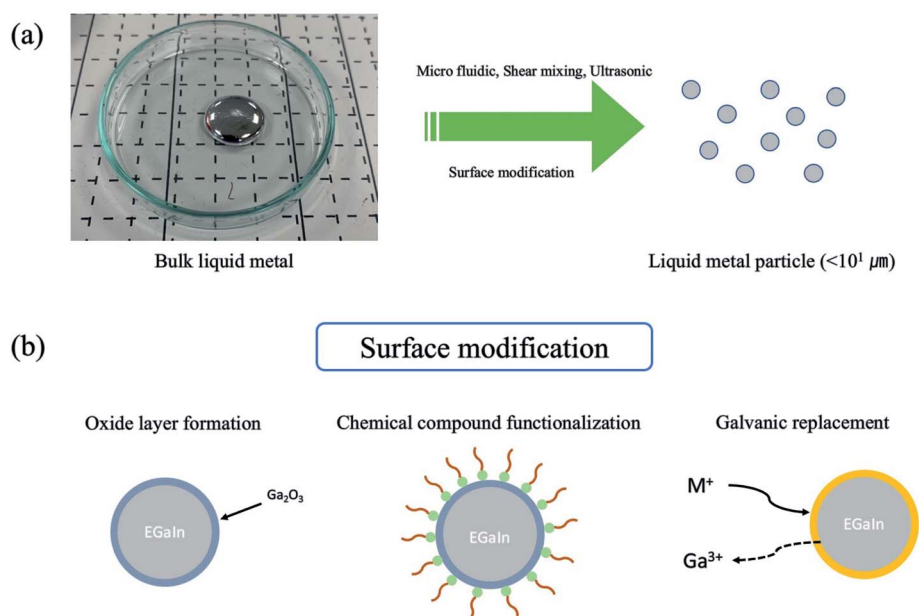

Fig. 1 Schematic illustration of (a) preparing liquid metal particles, and (b) surface modification of the liquid metal particles.

but low toxicity hazard, Ga has been widely used in various fields. In addition, Ga can be alloyed with other metals such as In, Sn, Al, Zn, Hg, or Ag, and the alloy has a lower melting point than Ga.[55] Furthermore, depending on the composition of the elements, the melting point is determined. For example, binaries of the Ga-based alloy have various melting points as a function of the atomic fraction. Based on the phase diagram of the Ga–In, 21.4 weight percentage (wt%) of In in the alloy showed lowest 288.3 K of eutectic temperature.[56] Currently, the Ga (78.6 wt%)–In (21.4 wt%) alloy is commercialized and called as eutectic GaIn (EGaIn). The Ga–Sn alloy showed the eutectic temperature at 293.7 K with Ga (87.6 wt%)–Sn (12.4 wt%).[57] In addition, the ternary alloy with Ga–In–Sn has been used as liquid metal at room temperature. In particular, the eutectic temperature of the ternary Ga (59.6–67 wt%)-In (20.5–26 wt%)–Sn (12.5–14.4 wt%) is in the range of temperature between 278 and 283.7 K.[58] These liquid metals have a liquid phase at near room temperature. Moreover, the high charge density near the Ga atoms in the liquid metal[59] endowed the high electrical conductivity of the liquid metal. Thus, the eutectic liquid metal is suitable for deformable and flexible electric devices. Based on the aforementioned properties, the basic properties of various liquid metals, which are in the liquid phase near room temperature, are compared in Table 1.

3. Surface modification of the liquid metal particle

3.1. Oxide layer formation on the liquid metal particle surface

Under ambient conditions, the surface of the liquid metal is naturally formed with a thin oxide layer, which is composed as gallium oxide (Ga_2O_3) and the thickness of that is normally 0.7–3 nm.[60,61] This oxide layer protects the bulk liquid phase, and that determines the shape of the liquid metal.[13,62] When the bulk scale liquid metal ($\sim 10^0$ mm) is exposed by an acid or base solution such as HCl or NaOH, respectively, the oxide layer is removed and the sphere shape of the liquid metal can be obtained due to the high surface tension, as shown in Fig. 2(a).[20] In addition, the oxide layer in NaOH can be controlled by the electrochemical potential, resulting in a shape change of the liquid metal.[13,63] Since the oxide layer on the liquid metal surface mechanically stabilizes the shape of the liquid metal, a smaller size of liquid metal particles produced by disassembling the bulk liquid metal can be obtained with the formation of a new oxide layer on the surface. For example, when the bulk liquid metal passed through a microfluidic channel in the oxygen-containing solution, the non-spherical liquid metal

Table 1 Physical properties of liquid metal at room temperature[59,114–116]

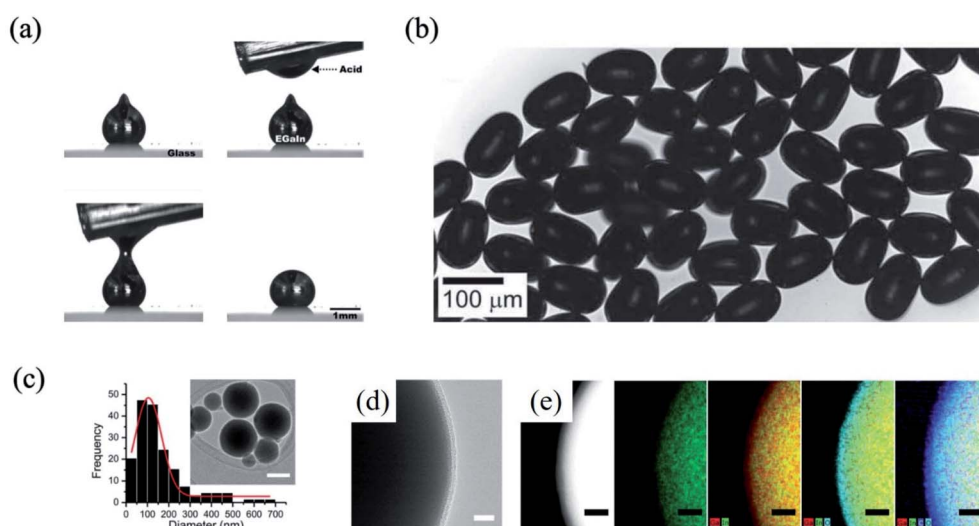| Materials	Hg	Ga	EGaIn	EGaInSn
Density (g cm^{-3})	13.53	6.08	6.28	6.36
Melting point (K)	234	303	288.5	283.5
Electrical conductivity (S m^{-1})	10 400	3.7×10^6	3.4×10^6	3.1×10^6
Thermal conductivity (W mK^{-1})	7.8	~ 30	~ 26	~ 25
Remark			Ga: 75.5%, In: 24.5%	Ga: 67%, In 20.5%, Sn: 12.5%

Fig. 2 (a) As dropped liquid metal with oxide layer generation, and removing the oxide layer by acid. Reproduced with permission from ref. 20. Copyright 2014, American Chemical Society. (b) Liquid metal particles produced by microfluidics. Reproduced with permission from ref. 22. Copyright 2012, John Wiley and Sons. (c) Size distribution and TEM image of liquid metal particles produced by ultrasonic method in ethanol, (d) liquid metal particle with ~3 nm oxide layer (scale bar: 5 nm), and (e) EDS mapping image of the liquid metal particle. Reproduced with permission from ref. 60. Copyright 2015, John Wiley and Sons.

particles, which are of ~10^2 µm in scale, can be obtained[22] (Fig. 2(b)). During the flow of the liquid metal, an instant oxide layer is generated on the small liquid metal particles, and the stabilized shape of the liquid metal particles is obtained without coalescence. Smaller liquid metal particles, which have the size distribution of ~10^2 nm, are produced by ultrasonic process (Fig. 2(c)). In smaller liquid metal particles, ~3 nm of the oxide layer is generated (Fig. 2(d) and (e)), and the liquid metal is stable in an organic solvent, such as ethanol or acetone. From the process, the bulk liquid metal is converted into liquid metal particles due to the generation of a new oxide layer on the surface of the liquid metal particles.[38,60,64] In this case, the oxide layer on the liquid metal plays not only the role of a protecting layer of the liquid GaIn, but also the role of a surfactant in ethanol.[60]

3.2. Chemical compound-assisted surface modification

The prepared liquid metal particles, which form an oxide layer in organic solvent, tend to be precipitated in organic solvent. In order to obtain the well-dispersed colloidal suspension, chemical compounds such as surfactants, thiol-containing molecules, phosphonic or carboxylic acid functionalized molecules or polymers were incorporated to help stabilize the liquid metal particles dispersed in the suspension.[16,27,28,30,35,65–69] For instance, liquid metal particles with

~10^2 nm of diameter can be obtained by ultrasonic dispersion method in ethanol containing 1-dodecanethiol.[27] During the ultrasonic process, 1-dodecanethiol tends to be a self-assembly monolayer on the surface of liquid metal particles. Even though the rapid oxidation on the surface of the liquid metal particles is generated,[66] the partial self-assembled monolayer helps the liquid metal particles dispersed in organic solvent, and kept as a stable suspension[27] (Fig. 3(a)). In addition, the interaction between the oxide layer and acid functional group-containing molecules provides well-dispersed liquid metal particles. In metal oxide nano-particles, functional ligands such as organo-phosphates or carboxylates have helped the metal oxide nanoparticles to be stable and prevent aggregation in the suspension. This is because the ligands are chemisorbed with strong binding to the metal oxide surface.[31,32,70–73] Likewise, when the bulk liquid metal was conducted using an ultrasonic process in a solvent containing molecules that have organo-phosphates or carboxylates, the oxide layer on the liquid metal particles (Ga_2O_3) has strong binding with the phosphate group or carboxylic acid group[15,28,30,74] (Fig. 3(b) and (c)). Besides, hydroxy groups are present in dopamine or amine group-containing molecules, such as *p*-phenylenediamine, that can be functionalized on the surface of the liquid metal.[75,76] These functionalized liquid metal particles are stable in the organic
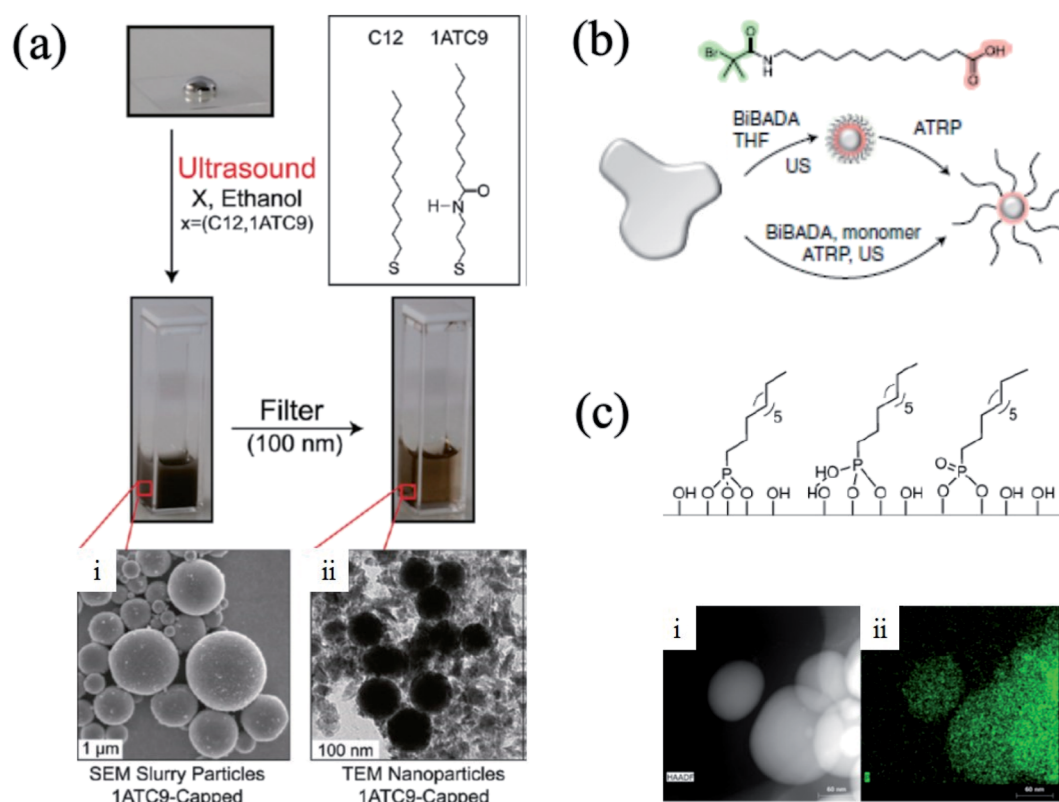

Fig. 3 (a) Thiol group functionalized liquid metal particle. Reproduced with permission from ref. 27. Copyright 2011, American Chemical Society. (b) Schematic illustration of the carboxylic group functionalized liquid metal particle. Reproduced with permission from ref. 30. Copyright 2019, Springer Nature. (c) Phosphate group functionalized liquid metal particle (scale bar: 60 nm). Reproduced with permission from ref. 74. Copyright 2018, American Chemical Society.

solvent as a colloidal suspension. In addition, liquid metal colloidal particles can be prepared by metal–organic frameworks such as zolitic imidazolate framework (ZIF-8) encapsulation. Liu *et al.* reported on the liquid metal particle/poly(vinyl pyrrolidone)/ZIF-8 core–shell composite.[77] In this case, ZIF-8 was crystalized near the liquid metal particles, and can be stabilized by poly(vinyl pyrrolidone). Since the metal–organic framework captured the liquid metal particles, the configuration between the ligand and metal ions of the metal–organic framework determined the sizes and structure of the particles.

3.3. Galvanic replacement

Galvanic replacement in liquid metal indicates that Ga atoms in the liquid metal can be replaced by metals such as Au, Ag, or Pt by electrochemical reaction. Generally, the reaction occurs in aqueous solution containing a metal salt. In the case of eutectic GaInSn, the standard reduction potentials of $Ga^{3+} + 3e^- \rightarrow Ga$, $In^{3+} + 3e^- \rightarrow In$, and $Sn^{2+} + 2e^- \rightarrow Sn$ are -0.529, -0.340, and -0.138 V, respectively, whereas those of $Ag^+ + e^- \rightarrow Ag$, $Au^+ + e^- \rightarrow Au$, and $Pt^{2+} + 2e^- \rightarrow Pt$ are 0.799, 1.83, 1.188 V, respectively.[18,78] In the components of the liquid metal, the standard reduction potential of Ga is the lowest. Hence, the galvanic replacement of Ga with Ag^+, Au^+, or Pt^{2+} is more likely than that of In or Sn. When the liquid metal particles are prepared by ultrasonic process in a metal ion (Ag^+, Au^+, or Pt^{2+})-containing aqueous solution, some Ga^{3+} ions participate in the oxidation and form Ga_2O_3 on the surface of the liquid metal particles, and metal ions (Ag^+, Au^+, or Pt^{2+}) dissolved in the aqueous solution are reduced into metals such as Ag, Au, or Pt, and are decorated on the surface of the liquid metal particles.[17–19,79,80] These prepared liquid metal particles have a core (Ag, Au, or Pt)–shell (GaInSn) structure, and these particles are stable in aqueous solution (Fig. 4). Furthermore, redox active mediators such as hexaammineruthenium(III) chloride ($Ru(NH_3)_6Cl_3$) and potassium ferricyanide(III) ($K_3Fe(CN)_6$) also reacted with GaInSn. Since the standard reduction potential of $Ru(NH_3)_6^{3+} + e^- \rightarrow Ru(NH_3)_6^{2+}$ and $Fe(CN)_6^{3-} + e^- \rightarrow Fe(CN)_6^{4-}$ is 0.1 and 0.361 V, respectively, the reduction reaction could occur on the liquid metal.[78,81] In the case of the redox active mediators, the result of the reaction causes the color change. For instance, the $Ru(NH_3)_6^{3+} + e^- \rightarrow Ru(NH_3)_6^{2+}$ and $Fe(CN)_6^{3-} + e^- \rightarrow Fe(CN)_6^{4-}$ cause the color to change from clear to red, and from yellow to green/blue, respectively.

4. Tailoring the physical and chemical properties of the liquid metal-based composites

4.1. Polymer matrix for composites with liquid metal

Applying the liquid metal in the flexible or deformable electronics, dispersion of liquid metal particles in a polymer matrix is an important consideration. Depending on the application of the liquid metal particles and polymer composite, the selection of polymer or fabrication process is different. The formation of composites between the liquid metal particles and elastomer has been actively studied. For example, the preparation of liquid metal particles and PDMS was conducted by shear mixing method. In this case, the uncured PDMS was shear-mixed with bulk liquid metal. During the shear mixing, the bulk liquid metal is divided
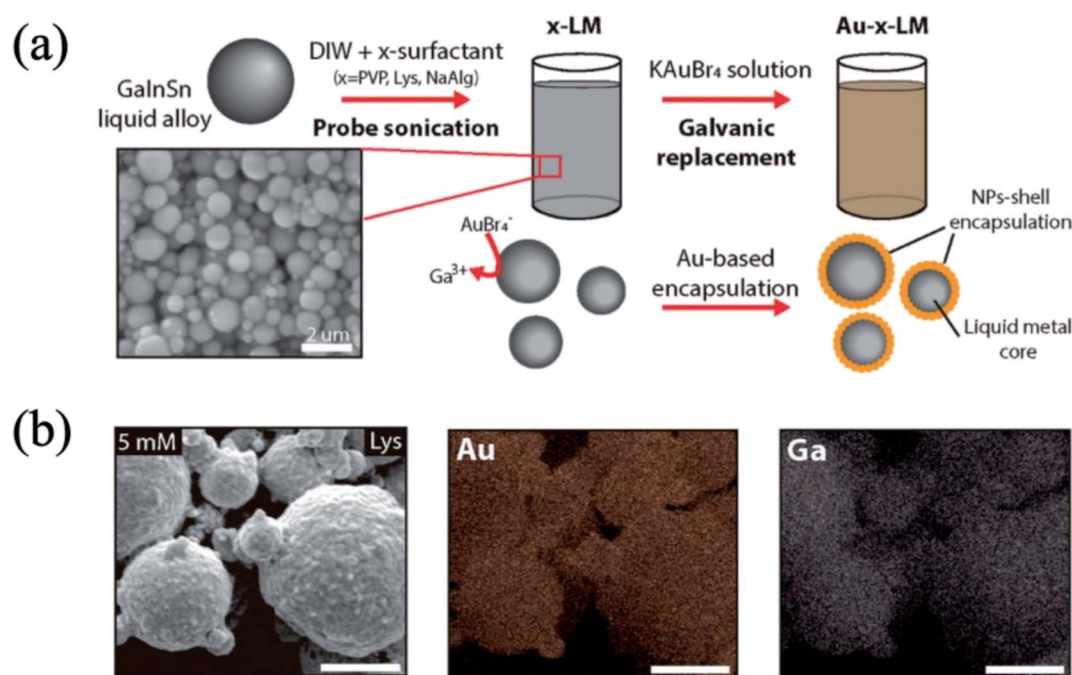

Fig. 4 (a) Schematic illustration of liquid metal particle preparation by galvanic replacement, and (b) SEM image and EDS mapping of the liquid metal particle (core) − Au (shell) (scale bar: 1 μm). Reproduced with permission from ref. 79. Copyright 2019, Royal Society of Chemistry.

into $\sim 10^1$ μm of liquid metal particles.[38,64,82] In addition, for the small size of the liquid metal particles ($\sim 10^2$ nm), the liquid metal particles are dispersed in solvent containing uncured PDMS by ultrasonic process[38,64] (Fig. 5(a)). The adhesion between the oxide layer formed on the surface of the liquid metal particles and the PDMS matrix is governed by solid–solid contact.[62] The contact angle between the liquid metal with the oxide layer and PDMS is lower than that between the liquid metal without an oxide layer,[83] which indicates that the wettability of the liquid metal in PDMS was improved by the oxide layer. However, in the case of the small size of liquid metal particles ($\sim 10^2$ nm), due to the large surface area, the large amount of the liquid metal particle loading (>20 vol%) is hard to disperse in the PDMS matrix.[38]

Another way to prepare the liquid metal and polymer composite is polymerization on the surface of the liquid metal particles. Since the oxide layer on the liquid metal particles have strong binding with molecules containing a carboxylic acid group or organo-phosphates, the polymerization on the surface of the liquid metal particles has been introduced. For example, Yan et al. introduced the surface-initiated atom transfer radical polymerization method[30] (Fig. 5(b)). In detail, 12-(2-bromoiso-butyramido)dodecanoic acid (BiBADA) served not only as a surfactant, but also as an initiator for the polymerization role on the liquid metal particles. As shown in Fig. 3(b), the BiBADA has a carboxylic acid group in the molecule, which interacts with the oxide layer on the liquid metal. After dispersion of the liquid metal particles in the organic solvent with the ultrasonic method, the initiator-functionalized liquid metal particles were prepared first. Using these initiator-functionalized liquid metal

particles, poly(methyl methacrylate) (PMMA), poly(n-butyl acrylate) (PBMA), poly(2-dimethylamino ethyl methacrylate) (PDMAEMA), and poly(n-butyl acrylate-block-methyl methacrylate) (PBA-b-PMMA) were synthesized on the surface of the liquid metal particles. Conversely, there is a surface functionalization with the monomer on the liquid metal particles. Thrasher et al. conducted the polymerization on the liquid metal particle surface with 11-phosphonoundecyl acrylate[15] (Fig. 5(c)). In 11-phosphonoundecyl acrylate, one end of the monomer has a phosphonic acid group, which has strong binding with the oxide layer on the liquid metal particles. On the other end, the acrylate group exists, and is able to be photo-polymerized. After the dispersion of the liquid metal particles with 11-phospho-noundecyl acrylate, poly acrylate and the liquid metal particles composite are prepared by photo-polymerization. In this case, the higher ratio of the liquid metal particles in the composite (>99 wt%) can be obtained. This is because the monomer is covering the liquid metal particles and the polymerization could occur at the monomer. Zhang et al. reported the surface polymerization on the liquid metal with p-phenylenediamine, which is a co-monomer of polyaniline.[75] In this case, the p-phenylenediamine played the role of a stabilizer of liquid metal particles due to the hydrogen bonding between the amine functional group in p-phenylenediamine and oxygen in Ga_2O_3, which is formed on the surface of the liquid metal particles. The surface-functionalized co-monomer and aniline monomer were polymerized on the surface of the liquid metal. In addition, Gan et al. fabricated polydopamine-coated liquid metal particles with surface polymerization.[76] Employing the ultrasonic method,
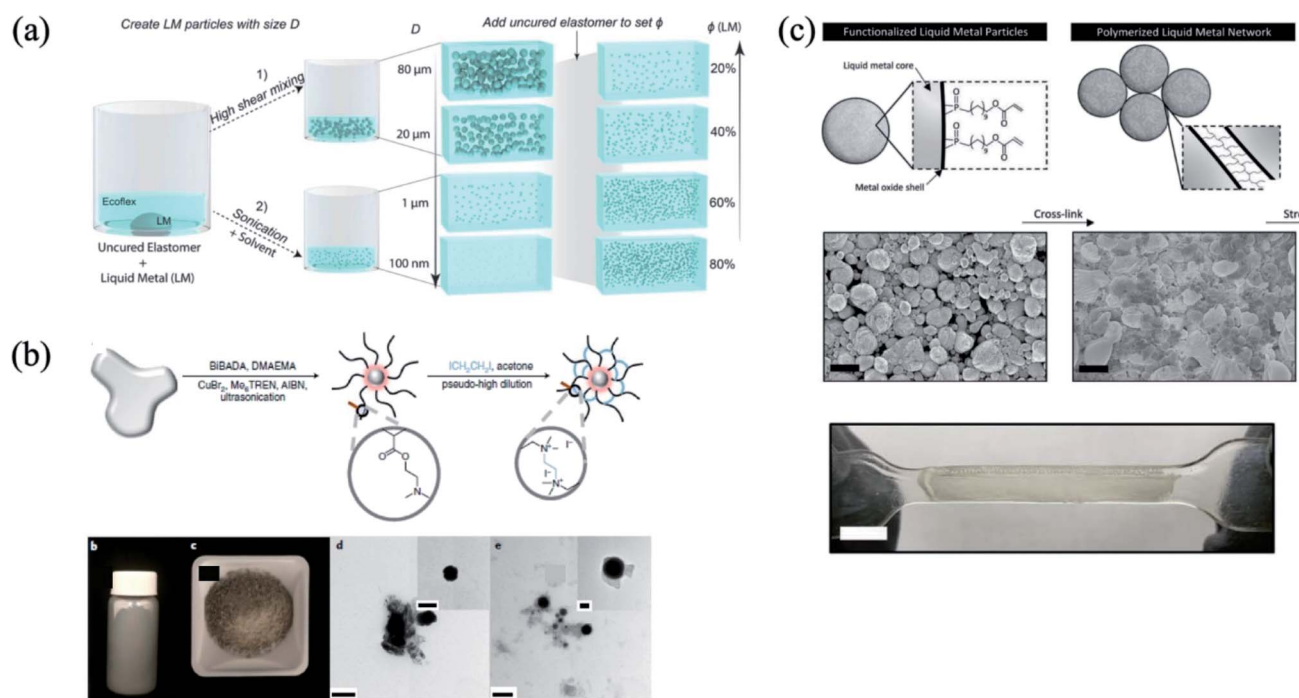

Fig. 5 (a) Preparation of the liquid metal/PDMS composite by shear mix ($\sim 10^1$ μm), or ultrasonic process ($\sim 10^2$ nm). Reproduced with permission from ref. 38. Copyright 2019, American Chemical Society. (b) Surface initiated polymerization on the liquid metal particle. Reproduced with permission from ref. 30. Copyright 2019, Springer Nature. (c) Photo-polymerized liquid metal particle. Reproduced with permission from ref. 15. Copyright 2019, John Wiley and Sons.

dopamine monomers were functionalized on the liquid metal particle, and the coalescence of the particles were prohibited by the monomers. After adding an initiator into the colloidal suspension, the polydopamine was polymerized on the surface of the liquid metal particles.

4.2. Physical and chemical interactions between the polymer matrix and liquid metal

Typically, in order to enhance the interaction between the rigid inorganic nanomaterials and polymer composite, the functionalization of the nanomaterials with organic ligand or organic compounds has been exploited.[84,85] However, since the liquid metal is in the liquid phase, the interfacial interaction between the liquid metal particles and polymer is distinctive in the composite formation, compared to the rigid filler such as inorganic nanomaterials and polymer composite. In the case of the liquid metal particles and PDMS elastomer composite, the oxide layer on the surface of the liquid metal particles influences the mechanical performance of the composite. For instance, Pan *et al.* reported the elastic modulus change of the liquid metal particles and PDMS composite as a function of the liquid metal
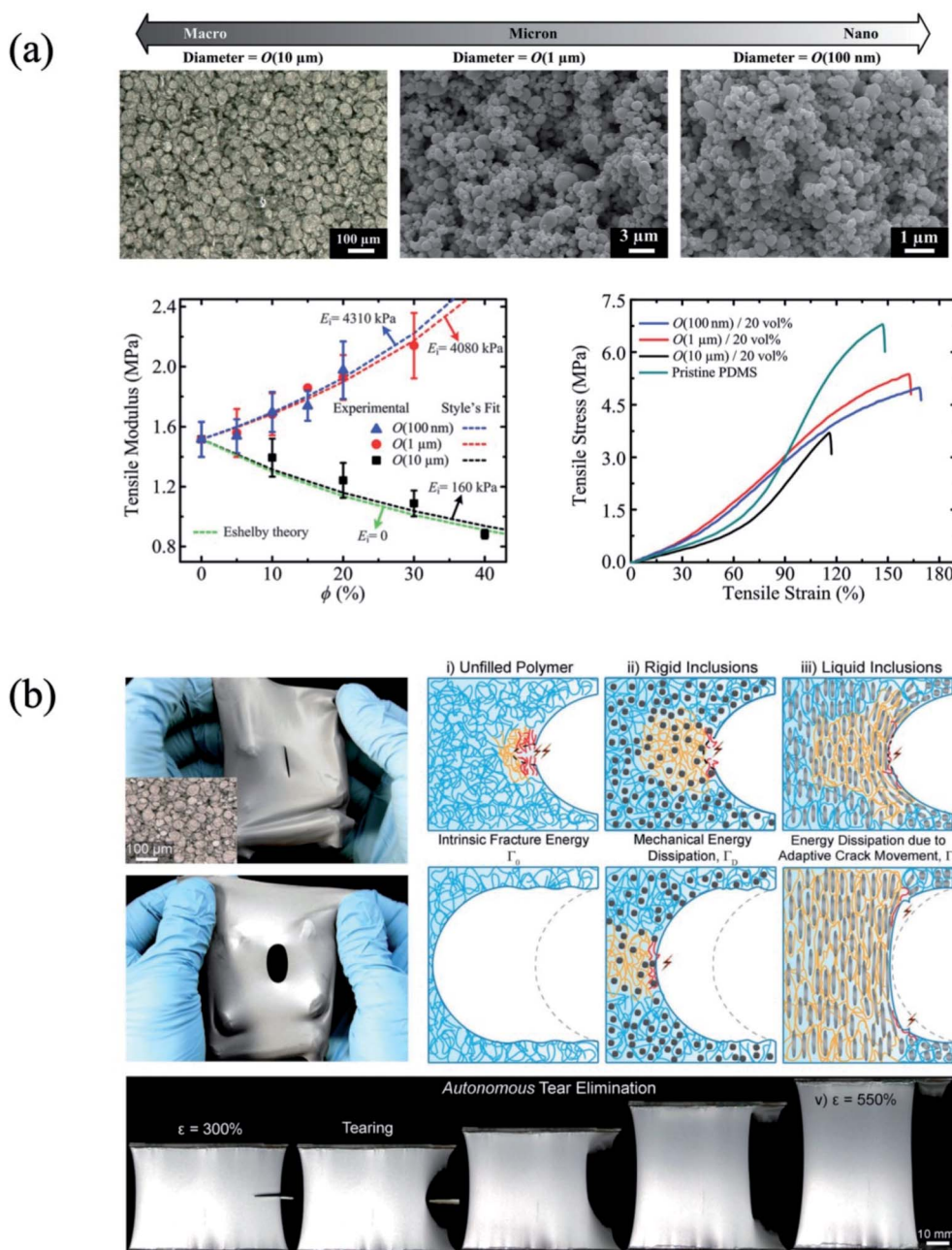

Fig. 6 (a) Mechanical performance of the liquid metal/PDMS composite depending on the liquid metal particle size. Reproduced with permission from ref.[64]. Copyright 2019, John Wiley and Sons. (b) High toughness mechanism of the liquid metal particle ($\sim 10^1$ μm)/PDMS composite. Reproduced with permission from ref. 86. Copyright 2018, John Wiley and Sons.

particle size.[64] Since there are smaller liquid metal particles ($\sim10^0$ µm) with a large surface area of oxide layer, the higher resistance to deformation resulted from the composite containing smaller particles. For example, the elastic modulus of the pure elastomer was 1.51 MPa, whereas that of the composite with 100 nm and 1 µm of liquid metal particles was 4.31 and 4.08 MPa, respectively (Fig. 6(a)). In the case of liquid metal particles functionalized with poly(n-butyl methacrylate) from surface-initiated polymerization,[30] the enhancement of the elastic modulus has been shown. With the strong interaction between the carboxylic acid group of the initiator with the surface oxides on the liquid metal particles, the polymerized composite has a higher stiffness. On the other hand, the elastic modulus of the composite with 100 µm of liquid metal particles was 0.16 MPa.[64] Even though liquid metal particles with a larger size ($\sim10^1$ µm) also have an oxide layer on the surface, the smaller interfacial area between the oxide layer and polymer matrix provided a smaller elastic modulus. In addition, due to the liquid phase in the core part of the liquid metal (inside the oxide layer), the liquid metal particles can be readily deformed under an external force.[39,86] For example, when the PDMS/liquid metal composite is strained, the shape of the liquid metal particle is deformed with a needle shape, which is aligned with the parallel direction of the strain. The deformed liquid metal particles deflect the crack movement, resulting in the toleration from the mechanical damage (Fig. 6(b)). In other words, this deformation of the liquid metal particles in the polymer matrix provides a higher fracture energy at higher strain, resulting in higher toughness.[86]

4.3. Electrochemical properties of the liquid metal particles and composites

Ga is readily reactive in acidic or alkaline medium, and the reaction is reversible between gallium and gallium oxide formation. Depending on the degree of pH, the Ga can be formed as $Ga + 3H_2O \leftrightarrow Ga(OH)_3 + 3H^+ + 3e^-$ (pH < 13), and $2Ga + 3H_2O \leftrightarrow Ga_2O_3 + 6H^+ + 6e^-$ (pH > 13).[87] Thus, the Ga-based liquid metal is electrochemically reactive. The presence of a thin native oxide layer on the surface of the liquid metal affects the interfacial tension, which can be controlled by the

electrochemical reaction.[11,13] The formation of the oxide layer is reversible as a function of the potential, resulting in a tunable surface tension of the liquid metal. In addition, as introduced above, liquid metal (eutectic GaIn) is composed of Ga and In, which has the standard reduction potential with −0.529 and −0.340 V, respectively.[78] Because of the low standard reduction potential of Ga, the liquid metal interacts electrochemically with the metal ion in solution. For example, the Fe particles and eutectic GaIn reacted in HCl or NaOH solution[88] (Fig. 7). Since the standard reduction potential of Fe^{2+}/Fe is −0.44 V, the Ga atom is converted into a Ga^{3+} ion via the $Ga \rightarrow Ga^{3+} + 3e^-$ reaction in HCl solution, and the Fe particles receive electrons, followed by the production of H_2 gas on the Fe particles. In the case of the reaction in NaOH solution, the reaction occurred as $2Ga + 2OH^- + 6H_2O \rightarrow 2[Ga(OH)_4]^- + 3H_2$. Due to the difference of the standard reduction potential between Ga and Fe, the galvanic reaction is generated naturally, and the Ga^{3+} ion is increased as a function of time at room temperature.[88] Besides, the role of In in the eutectic GaIn is electrochemically important. Liu et al. reported the usage of eutectic GaIn as an anode in a battery.[89] In the anode part, the reaction occurred as $Ga + In^{3+} \rightarrow Ga^{3+} + In$. Even though Ga is readily corrosive in KOH solution, In prevents Ga from corrosion because In has a high hydrogen overpotential.[90]

5. Applications of the surface-modified liquid metal particles

5.1. Flexible and stretchable conductors

Owing to the low resistivity and deformable structure, liquid metal is promising as a core material for flexible or stretchable conductors. In the case of the surface-functionalized liquid metal particles, since the particles are well-dispersed in an organic solvent, a flexible or stretchable electrode can be obtained by the solution process. As discussed above, the surface-functionalized liquid metal with a thin oxide layer or chemical compound showed stability in an organic solvent. For example, Lin et al. prepared ~100 nm of a liquid metal particle suspension in ethanol, which was fabricated by ultrasonic process.[60]
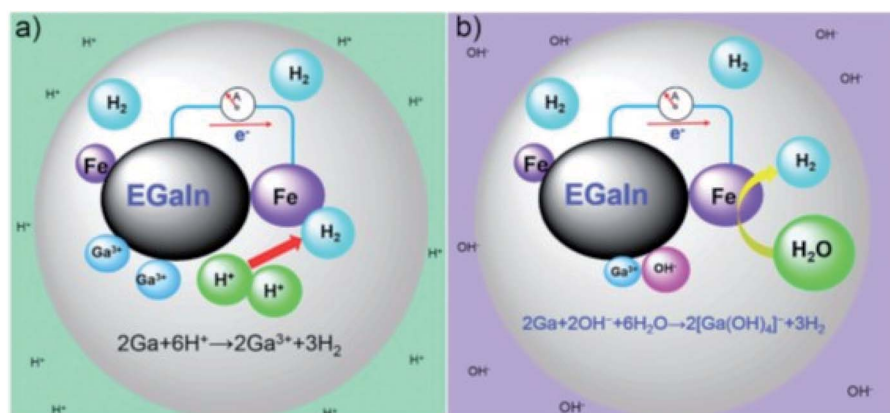

Fig. 7 Schematic illustration of the electrochemical reaction between the liquid metal and Fe in (a) HCl and (b) NaOH. Reproduced with permission from ref. 88. Copyright 2017, Royal Society of Chemistry.
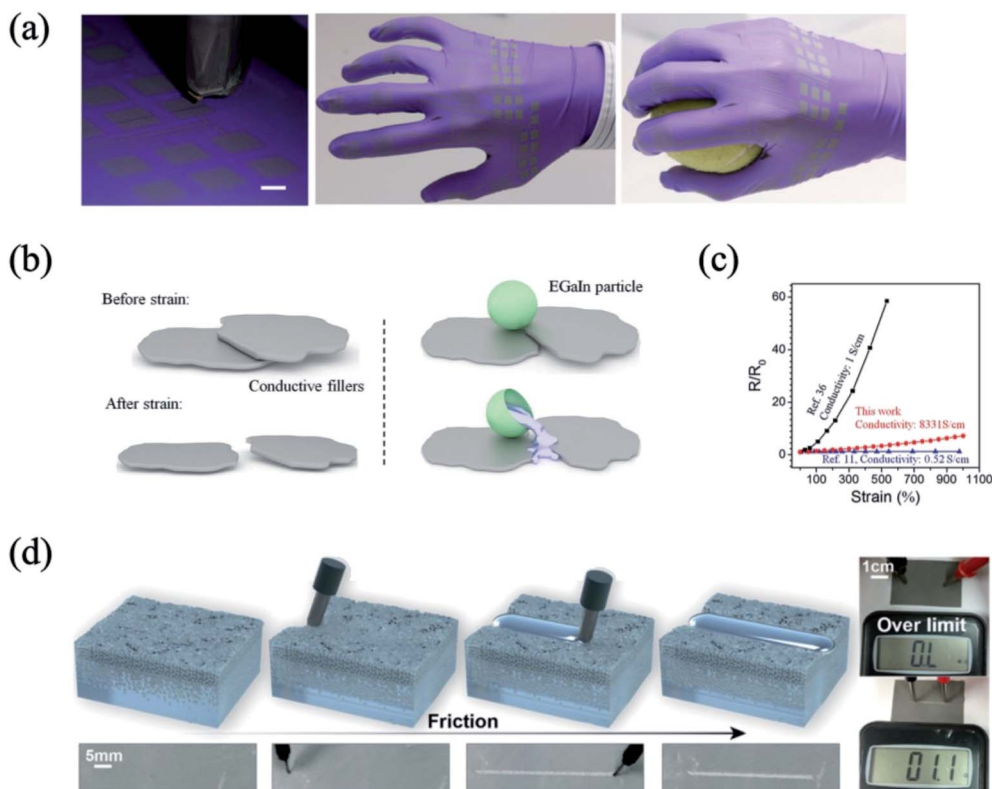
Fig. 8 (a) Ink-jet printed colloidal suspension with liquid metal particles on a polymer glove. Reproduced with permission from ref. 35. Copyright 2015, John Wiley and Sons. (b) Concept of the liquid metal particle as an electrically conductive bridge between metal fillers, (c) sustainable resistance as a function of strain in the Ag flake/liquid metal particle/EVA composite. Reproduced with permission from ref. 25. Copyright 2018, John Wiley and Sons. (d) Electrically conductive path generation from mechanical force. Reproduced with permission from ref. 93. Copyright 2019, American Chemical Society.

Boley *et al.* prepared a well-dispersed suspension of liquid metal particles functionalized with thiol compound molecules in ethanol.[35] The prepared suspension was dropped or ink-jet printed on the flexible substrate, such as polymer glove (Fig. 8(a)). However, since the oxide layer on the liquid metal (Ga_2O_3) has a high band gap,[91] there is the loss of electrical conductivity with the as-prepared flexible electrode. The oxide layer fractures readily under a mechanical force, and the liquid phase in the oxide layer coalesces and provides an electron transport path. However, the higher extent of chemical functionalization on the liquid metal particle surface can generate the electrical resistance in the patterned electrode. The chemical functional compounds are important in controlling the size of the liquid metal particles under 10^2 nm. Although the higher extent of chemical functionalization may provide smaller size of liquid metal particles, which can be precisely patterned, the higher resistance of the electrode could entail. In the case of the larger size liquid metal particles ($\sim 10^1$ μm), the liquid metal particles have electrically healable characteristics. Blaiszik *et al.* prepared the line-patterned Au electrode, and the oxide layer-covered liquid metal particles were dropped on the electrode.[92] When the electrode was damaged, the liquid metal particle was also fractured and the liquid phase of the liquid metal was spilled out, resulting in covering the damaged site. In the preparation of the stretchable electrode, generally, metal

fillers are dispersed randomly in the polymer matrix. Upon stretching, the electrical performance is typically deteriorated due to the poor inter-connection of the metal fillers. Addition of liquid metal particles in the composite provides an advantage of sustainable electrical conductivity at high strain. Wang *et al.* reported on the Ag flake/liquid metal particles/ethylene vinyl acetate (EVA) composite for a stretchable electrode[25] (Fig. 8(b)). Under strain, the liquid metal particles were broken and the liquid phase played the role of electron transport bridges. Hence, the percentage of resistance fluctuation was sustained below 10% at 1000% of strain (Fig. 8(c)). In addition, the Ni flake/carboxylic polyurethane/liquid metal particle composite showed a similar tendency.[24] Notably, the composite is a self-healing material due to the hydrogen bonding in the polymer matrix. Even though the composite was cut and self-healed, the resistance was sustained as a function of strain. In the case of the liquid metal and polymer composite, normally, the liquid metal particles dispersed in a polymer matrix with $\sim 10^1$ μm of size have no electrical conductivity. However, the locally sintered liquid metal particles in the composite provide new electrically conductive pathways.[34,36,93,94] In detail, when the composite was damaged by cutting or tearing, or it was locally pressed, the liquid metal particles near the site were merged, and provided an electron transport path (Fig. 8(d)). Therefore, even though the composite is physically damaged, the electrical

conductivity can be sustained by the coalescence of the broken liquid metal. By exerting mechanical pressure on the liquid metal particles/polymer composite, the customized pattern of the electrically conductive circuit can be formed.[60,93] On the other hand, in the case of the smaller size of the liquid metal particles ($<10^2$ nm), a higher volume loading (>20 vol%) of liquid metal particles is limited due to the brittle behavior of the resulting composite, caused by the difficulty in wetting the high volume fraction of the liquid metals.[38] Thus, the size control of the liquid metal particles is significantly important in the liquid metal/polymer composite for the flexible or deformable electrode application.

5.2.   Soft robotics

The surface charged or metal (semiconductor) decorated liquid metal has considerable potential in soft robotics. There have been several reports about the manipulation of the liquid metal triggered by an electric field, catalytic reaction, and magnetic field. Generally, in alkali solutions such as NaOH, the surface of the Ga-based liquid metal forms $Ga(OH)_4^-$, resulting in a negative charge in the solution, and an electric double layer is generated in the solution.[40] Based on the Lippmann equation, which shows the correlation between the surface tension and the potential difference across the electrical double layer, the distortion of the interfacial tension is generated by the electric field.[95] In addition, the electric field can be a driving force for the movement of the liquid metal in the alkali solution. The metal or semiconductor-decorated liquid metal is useful for the actuation of the liquid metal. For example, Gao *et al.* reported an actuation performance of the Ga–Al/Ti Janus particles in H_2O.[42] The prepared Janus particle can be mobile in aqueous solution because a water-splitting reaction occurred with aluminum and H_2O, as shown in the depicted equation: 2Al (s) + 6H$_2$O (aq) → 2Al(OH)$_3$ (s) +3H$_2$ (g)

Fig. 9   (a) Actuation performance of the WO$_3$ decorated liquid metal by photochemical reaction. Reproduced with permission from ref. 41. Copyright 2013, AIP publishing. (b) Manipulation and switch performance of the magnetic liquid metal. Reproduced with permission from ref. 44. Copyright 2016, Royal Society of Chemistry. (c) Schematic illustration of the cable type liquid metal (anode)−air battery. Reproduced with permission from ref. 89. Copyright 2018, John Wiley and Sons. (d) Self-healable and stretchable hybrid energy storage device. Reproduced with permission from ref. 24. Copyright 2018, John Wiley and Sons.

In this case, the hydrogen generation, which was produced at the Al–Ga part in the Janus particle, played a driving force for the Janus particles in aqueous solution. However, since this hydrogen gas generation is a spontaneous reaction in aqueous solution, it is hard to intentionally manipulate. In addition, owing to the water-splitting reaction between Al and H_2O, the movement of the particle is restricted by the amount of Al in the particle. In order to overcome this, a photocatalytic reaction can be employed. For instance, Tang et al. prepared WO_3-decorated liquid metal, and showed the actuation performance.[41] When the light source ($\lambda = 320$–380 nm) was applied to WO_3, photo-excitation occurred. In addition, in H_2O_2 solution, this photo-catalytic reaction decomposed H_2O_2 and produced O_2 gas. In the WO_3-decorated liquid metal, the O_2 gas, which was produced by photocatalytic reaction, can roll the liquid metal. Thus, depending on the light exposure, the oxygen gas generation can be controlled, and the oxygen gas can be the driving force of the movement of the liquid metal (Fig. 9(a)). Besides, the magnetic liquid metal can be manipulated intentionally with a magnet. The actuation performance of the liquid metal by the magnetic field has been shown with the Fe particle and liquid metal composite. The decoration of the Fe particles on liquid metal is readily prepared by rolling a droplet of liquid metal on the Fe particle bed,[44–46] or by mechanical stirring.[43] Since the Fe-doped liquid metal has electrical conductivity and the position of that is manipulated by the magnetic field, this actuation performance can be utilized for self-healing of the electrically conductive path.[43] When the physical damage was generated at the electrode, which is composed of Fe-decorated liquid metal, the split electrode can be recovered by the magnetic field due to the emerging liquid metal. Besides, the magnetic liquid metal can play a bridge role between the electrodes, which is a similar function of a switch. Positioning the disconnected gap between the electrodes by the magnetic field, the Fe-decorated liquid metal instantly provides the electrically conductive path (Fig. 9(b)).

5.3. Electrochemical energy storages

In the battery system, since the Ga forms alloys with the alkali ion, which has high capacity,[96] the battery field has focused on the liquid metal as an anode. For example, in the case of Ga, 2 Li atoms are formed with 1 Ga atom, and the formed Li_2Ga has a theoretical capacity of 768 mA h g^{-1}.[97] Besides, the Ga-based liquid metal can be a core material for interface engineering between the anode and current collector. In the Si anode-based Li ion battery, the delamination between the Si particles and Cu current collector was an issue. Employing the GaInSn liquid metal as a buffer layer between the Si particles and Cu current collector, the delamination was mitigated without sacrificing the capacity.[98] Additionally, the Ga-based liquid metal can enhance the performance of the current collector. The alloying $CuGa_2$ was found to break down the native oxide and enhanced the electron transfer ability in the current collector.[99] In addition, due to the low melting point of Ga at 29 °C, the anode part can be self-healed from the delithiation at room temperature. Considering the low melting point and deformable feature,

eutectic GaIn is also a promising material for energy storage. Liu et al. fabricated a cable-typed battery, which is composed of eutectic GaIn (anode), poly(acrylic acid)-based gel electrolyte, and Pt nanoflower-decorated carbon fiber yarn (cathode)[89] (Fig. 9(c)). Due to the liquid phase of the liquid metal, the shape of the anode part was recovered from the finger-pressure or strain. Among the cable-typed battery research, the eutectic GaIn anode showed the highest discharge performance with 0.265 mW cm^{-2} at 1.5 V. Liquid metal particles have been used in several examples for battery applications. Guo et al. reported the performance of the eutectic GaIn particles as an anode.[100] 200 nm of liquid metal particles was prepared by ultrasonic method, and the liquid metal particles were functionalized with sodium dodecyl sulfate. The liquid metal particles have a short ion diffusion length corresponding to their sizes, and the rate performance of the cell was improved when a high diffusion coefficient with $\sim 1.01 \times 10^{-7}$ cm^2 s^{-1} for Li was obtained. Park et al. have shown the promising performance of the hybrid-type stretchable energy storage device with the eutectic GaIn particle/Ni flake/self-healing polymer composite.[24] Employing the redox reaction of Ga^{3+}/Ga, the operation voltage of the device reached up to 3.5 V. After the charging device, the electric watch display was operated under strain at 200%. Interestingly, the capacity of the device was maintained to $\sim$76% after 5 cycles of self-healing time, which indicates that the electrochemical performance of the device was still sustained after self-healing recovery from repeated cutting of the device owing to the polymer matrix used (Fig. 9(d)).

5.4. Triboelectric energy harvesters

Due to the emerging wearable electronic devices, the demands of a deformable energy-harvesting device are necessitated. On this point, the liquid metal is also a useful material in the energy-harvesting field. In the triboelectric energy harvesting system, liquid metal particles can be used in the dielectric layer and current collector layer. First, there are examples of a liquid metal/PDMS composite for the dielectric layer in the triboelectric device[101,102] (Fig. 10(a)). In the case of the dielectric layer, the high surface charge density is an important part for enhancing the triboelectric performance. In addition, the liquid metal particles are shape-deformable. The liquid metal particles and PDMS composite showed deformability and durability from mechanical force, and their electrical properties are useful for the wearable triboelectric device (Fig. 10(b)). In the case of the dielectric layer, the smaller size and higher amount of liquid metal particles show that the higher triboelectric performance is due to the high dielectric constant. However, with the large amount of liquid metal loading in the PDMS matrix, the mechanical force in the liquid metal/PDMS composite caused the coalescence of the liquid metal particles, resulting in the charge leakage and high electrical conductivity. Similarly, the triboelectric performance of the electrospun polyacrylonitrile membrane was enhanced by liquid metal particle decoration.[103] However, the higher amount of liquid metal particle caused the increase of the electrical conductivity owing to the coalescence of the liquid metal particles, and the triboelectric performance deteriorated. In this
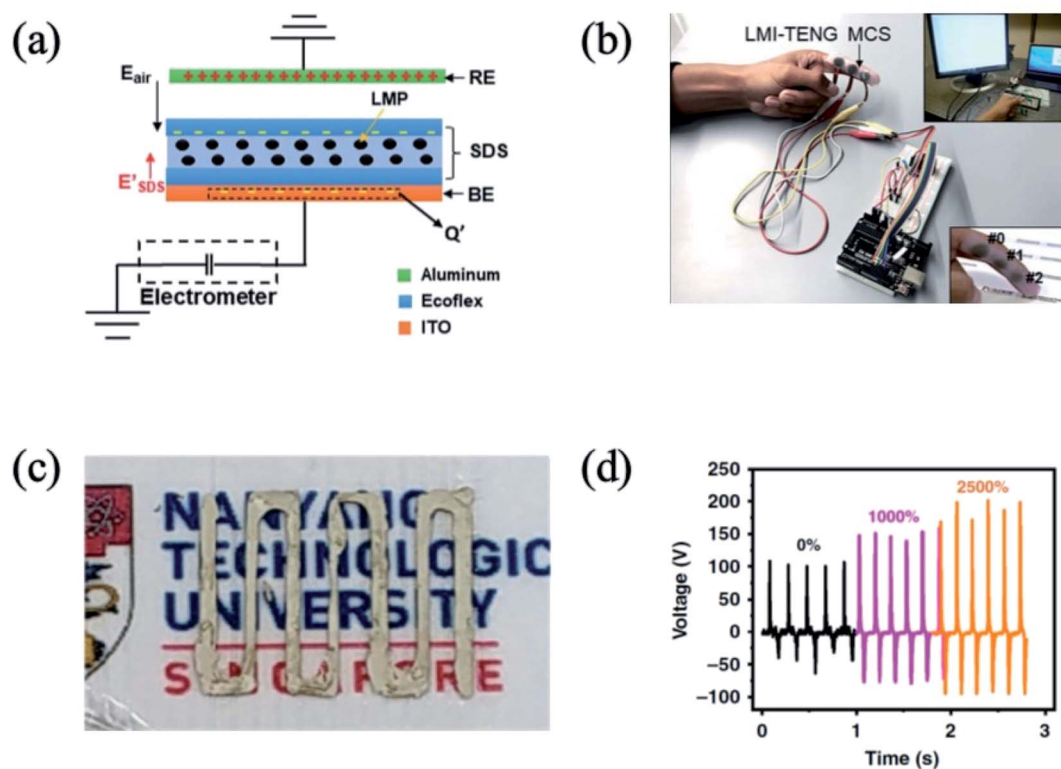
Fig. 10 (a) Schematic illustration of the triboelectric generator structure, (b) liquid metal/PDMS composite based wearable triboelectric device. Reproduced with permission from ref. 102. Copyright 2019 Royal Society of Chemistry. (c) Ag flake/liquid metal particle/carboxylic polyurethane composite based patterned triboelectric device, and (d) generated voltage of the Ag flake/liquid metal particle/carboxylic polyurethane composite based patterned triboelectric device as a function of strain. Reproduced with permission from ref. 104. Copyright 2019 Springer Nature.

perspective, preparing the dense and smaller size of liquid metal particles in the polymer composite is suitable for the dielectric material of the triboelectric device. Therefore, the functionalization of the liquid metal particles, such as surface-initiated polymerization of liquid metal particles, is required to prevent the coalescence of the liquid metal particles and prevent the deterioration of the dielectric constant.

Considering that the coalescence of a high amount of liquid metal particles would occur under mechanical force, which may lead to the formation of electrically conductive paths, the liquid metal can be a good current collector in the triboelectric generator. Parida et al. reported on a carboxylic polyurethane-based triboelectric generator.[104] When the current collector was fabricated with carboxylic acid polyurethane/Ag flake/liquid metal particles (Fig. 10(c)) and the triboelectric dielectric layer was composed of a carboxylic acid polyurethane layer, the maximum output voltage generated was up to 200 V at 2500% of the uniaxial strain (Fig. 10(d)) due to the anchoring role of the liquid metal particles in the composite under strain. Since well-dispersed liquid metal particles in PDMS have a high dielectric constant, the liquid metal particles can also be a good additive in the current collector part. Coupled with their structural deformation property, the liquid metal particle dispersed composite is a good candidate for wearable triboelectric energy harvesting.

5.5. Thermal conductive materials

As the Ga and In-based liquid metal has a high thermal conductivity with $\sim$26 W mK^{-1},[21] the liquid metal/polymer composite can be a good thermal conductive material. Mostly, the thermal conductive performance of the liquid metal particles and PDMS composite has been reported. In the case of the shear mixed eutectic GaInSn and PDMS composite, the thermal conductivity reached 2.2 W mK^{-1} with 92.5 wt% of eutectic GaInSn.[105] In addition, the filler composite, which is composed of liquid metal and Cu particle[106] or graphene nanoplatelets,[107] has been used for higher thermal conductivity ($\sim$10 W mK^{-1}). The liquid metal particle provides the phonon transport path between the other fillers, and the thermal conductivity can be enhanced. An interesting point of the liquid metal particle/PDMS composite is the anisotropic thermal conductivity as a function of strain. When the liquid metal particles/PDMS composite is strained, the directional thermal conductivity was changed. Bartlett et al. reported the anisotropic thermal conductivity of the liquid metal particle/PDMS composite.[39] As we discussed above, when the $\sim$10^1 μm size of the liquid metal is dispersed in the PDMS, the shape of the liquid metal is deformed into a needle shape under strain, and the deformed liquid metal particles were aligned with a parallel direction of the strain (Fig. 11(a)). In this case, the thermally conductive path was created along the strain direction. As a result, the
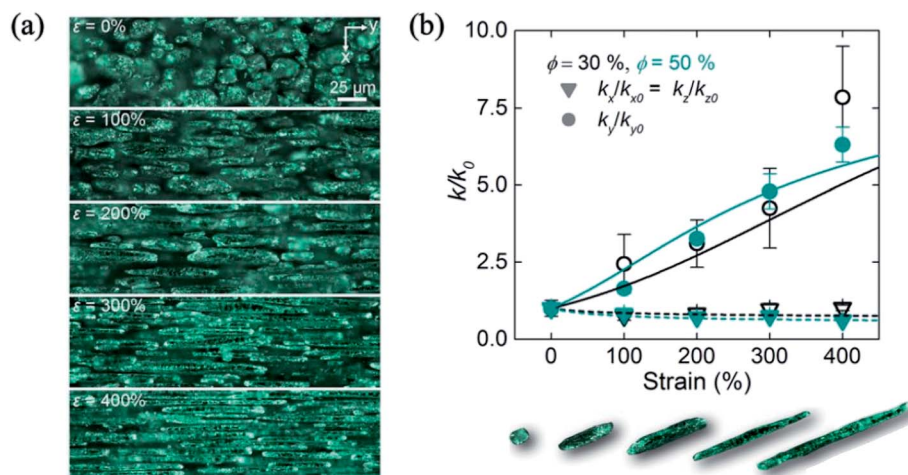
Fig. 11 (a) Deformation of the liquid metal particles in the PDMS matrix, and (b) anisotropic thermal conductivity of the liquid metal particles/PDMS composite as a function of strain. Reproduced with permission from ref. 39. Copyright 2017 National Academy of Sciences.

thermal conductivity of the parallel direction of strain was enhanced to 7.5 times higher from 0 to 400% of strain (Fig. 11(b)).

The thermally conductive composite can be used in thermoelectric devices. Since the thermoelectric power generation is generated by the temperature gradient between the hot side and cold side of the device, the delivery of the thermal stimuli on the hot or cold side determines the power output performance of the thermoelectric device. Typically, aluminum oxide has been employed for the thermal interface of the temperature gradient in the thermoelectric device. However, owing to the rigid and difficulty of deformation, there are limitations for the wearable thermoelectric device. Thus, a liquid metal particles-dispersed polymer composite can be a good thermal interface in the thermoelectric device. For example, Malakooti *et al.* reported that the liquid metal particles/PDMS composite can be used in the thermal interface of the thermoelectric device.[108] The commercial thermoelectric device was embedded in the PDMS, and the cold side and hot side of the aluminum oxide layer were covered with the liquid metal particles/PDMS composite. This device was employed for covering the whole human arm. However, since the device was prepared with the commercial thermoelectric device, which is rigid and not

deformable, the replacement of the aluminum oxide layer on the thermoelectric device is required. In this perspective, Zadan *et al.* developed a flexible thermoelectric device with a liquid metal particles/PDMS composite.[109] The liquid metal particles/PDMS composite was used as the hot side and cold side layers, which were typically aluminum oxide. Notably, the liquid metal particle/PDMS composite was used as not only the thermally conductive layer, but it also played the role of the local electrode in the thermoelectric device. As aforementioned, the mechanical force in the liquid metal particle/PDMS composite generates the coalescence of the liquid metal particles. In addition, the merged liquid metal particles provide an electrically conductive path. Thus, patterning on the liquid metal particle/PDMS composite, and the electrodes of the p- and n-type series connection can be prepared.

5.6. Dielectric materials

Liquid metal is also used as a capacitive sensor in the liquid metal/PDMS composite. Depending on the contacted surface area between the liquid phase metal, such as metal or dielectric materials, the capacitance can be changed.[110,111] Since eutectic GaIn is also deformable as a function of force, eutectic GaIn has been used in the capacitive sensor. Cooper
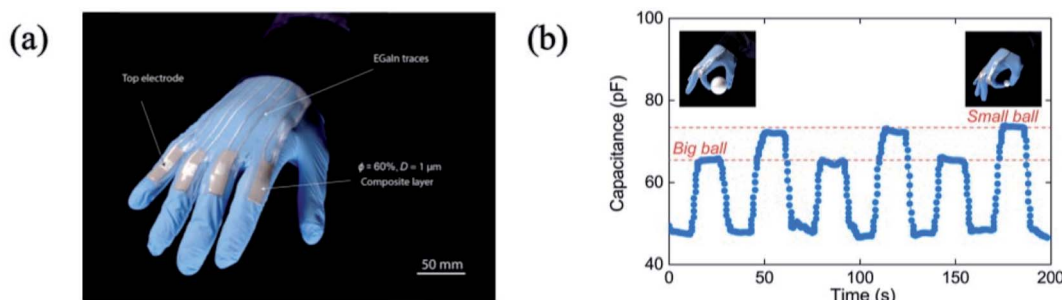

Fig. 12 (a) Prototype of the hand motion capacitive sensor, and (b) change of the capacitance depending on the gesture. Reproduced with permission from ref. 38. Copyright 2019, American Chemical Society.

et al. prepared a core (eutectic GaIn)–shell (PDMS) fiber, and the capacitance was changed as a function of force, such as torsion or strain.[112] In addition, Tutika *et al.* reported the oxide layer-formed liquid metal particles/PDMS composite, which has been used for the capacitive sensor.[38] When the composite is subjected to force, the shape of the liquid metal particles were locally changed, resulting in changes of the surface area. This phenomenon can be applied in a wearable capacitive sensor for the hand motion, such as the bending or strain of the finger[38] (Fig. 12(a) and (b)).

In addition, employing a dielectric layer with the liquid metal/PDMS composite, the dielectric elastomer actuator and dielectric elastomer generator can be utilized.[64] In the case of the actuation performance, due to the higher dielectric constant of the elastomer with the liquid metal particle, when the high voltage electric field was applied, the elastomer with the liquid metal particle showed a higher average blocking force than the elastomer without the liquid metal particles. Since the dielectric layer undergoes a change of electrostatic potential with mechanical deformation, the phenomenon can be utilized for the conversion from mechanical work to electrical energy.

5.7. Biomaterials

Chemical compounds supported with liquid metal particles can be used as biomaterials because of their low toxicity. Chemical functional groups containing a carboxylic acid group, thiol group, or phosphate group can be functionalized on the surface of the liquid metal particles.[15,27,30] For example, ∼10^1 nm scale of liquid metal particle functionalized with bio-polymeric materials showed promising result on the drug delivery application.[16,67,113] In this case, the functionalized particles are transported to a target point, such as a tumor, and the release of the drug is conducted by proton or local heat generation *via* light source. Since the surface of the liquid metal particles can be functionalized with chemical functional groups, such as thiol, phosphate acid, or carboxylic acid group, there is an opportunity to attach or chemically couple the drugs on the liquid metal surface (Fig. 13(a)). In addition, the liquid metal can be decomposed or shape-deformed depending on the pH or temperature, respectively, resulting in the drug release[16,65] (Fig. 13(b) and (c)).

6. Limitations and challenges

Although the surface-modified liquid metal particles have shown the potential for the various applications, several limitations and challenges still remain. For example, most of the research studies on the flexible electrode have been focused on the ∼10^1 μm scale of liquid metal particles. These several tens of micron scale of liquid metal particles provide the electrically
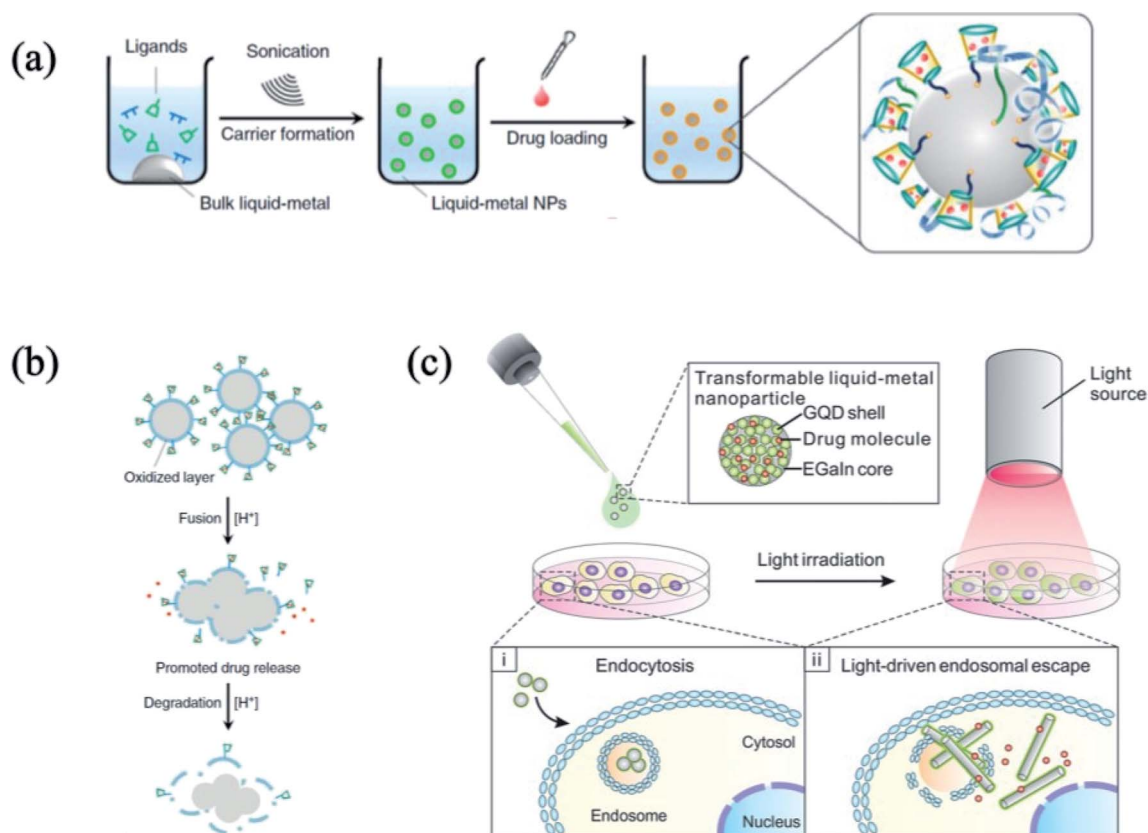

Fig. 13 (a) Schematic illustration of the drug delivery material preparation, and drug release mechanism by (b) proton assistance. Reproduced with permission from ref. 16. Copyright 2015 Springer Nature. (c) Shape deformation from IR. Reproduced with permission from ref. 113. Copyright 2017, American Chemical Society.

conductive path upon mechanical breakage of the oxide shell. However, a continuous mechanical force can generate an unintended electrically conductive path. In addition, the submicron scale patterning of the electrode is challenging. Even though the 10^1–10^2 nm scale of the liquid metal particles can be obtained by employing surface modification with chemical compounds, the precise patterning is limited. While the higher concentration of the chemical functional groups may lead to well-distributed liquid metal particles with smaller sizes (~10^1 nm), the chemical compounds may inhibit the electrical conductivity. In addition, the wettability and corrosive issue of the liquid metal remained unresolved. In order to remove the oxide layer on the surface of the liquid metal particles, an alkali or acidic-based solution was exploited for removing the surface oxides. After removing the oxide layer, the large surface tension of the liquid metal causes the conversion into a spherical bead shape. In this case, the poor wettability on the substrate is the issue for the utilization of the liquid metal. With the continuous exposure in alkali or acidic-based solution, corrosion of Ga may occur. Another challenge is the thermal issue. When the ambient temperature is increased to 343 K under ambient condition, the phase separation occurred and the liquid phase is converted into a crystalline structure (GaOOH). In this perspective, there is a possibility of the deterioration of the mechanical properties with the liquid metal/polymer composite under higher temperature. Last but not least, if considering the drug delivery by heating up the liquid metal particles containing the drug, the biological safety of the GaOOH, In, or Sn should be confirmed.

7. Summary and outlook

To sum up, we discussed the surface modification of the liquid metal particles and their applications. Due to the deformable feature, low toxicity, high electrical conductivity, and electrochemical performance of the liquid metal, the liquid metal is emerging as a core material for soft electronics, wearable devices, and energy storage or harvesting application. Generally, the bulk Ga-based liquid metal naturally forms the oxide thin layer (Ga_2O_3) on the surface. When the bulk liquid metal particles are subjected to a shear-mixing or ultrasonic process, the bulk liquid metal is separated into $\leq 10^2$ μm size and becomes stable due to the new oxide layer generation on the surface of the liquid metal particles. In addition, the oxide layer on the liquid metal particles interacts with chemical compounds, which contain carboxylic acid group, phosphate group, hydroxy group, amine group, thiol group, or metal–organic frameworks. Employing these chemical compounds and ultrasonic process, the colloidal suspension of liquid metal particles, which have ~10^2 nm size and are stable in organic solvent, can be obtained. Since these surface functionalizations of the liquid metal particles are solution-processable, the inkjet printing of the liquid metal particle colloidal solution and the composite preparation *via* surface-initiated polymerization can be practical. In addition, the spontaneous chemical reaction owing to the reduction potential between Ga and the noble metals makes it possible that the surface of the Ga-based liquid

metal particles can be decorated by noble metals, which has a core–shell structure. These functionalized liquid metal particles can be used in various applications. Owing to the infinite deformation of the liquid metal and high electrical conductivity, the surface-functionalized liquid metal particle and polymer composite can be a candidate of the flexible and stretchable electrode. However, even though the surface-functionalized liquid metal particles are well dispersed in the organic solvent or polymer matrix, the surface oxide layer, the chemical compound molecules or polymer may inhibit the electrical conductivity of the composite. Thus, the coalescence of the liquid phase in the surface-functionalized layer (such as Ga–In or Ga–In–Sn) is required by external mechanical force. For example, the local damage of the liquid metal particles/PDMS composite provided the electrically conductive path. When the ~10^1 μm size of the liquid metal particles was damaged, the oxide layer of the liquid metal particles was broken and the liquid phase of Ga–In or Ga–In–Sn was spilled and merged. This method is useful for the free drawing of the electrode pattern or stretchable conductors, but there is a possibility of the generation of unintended electrically conductive paths by the additional stress in the composite. In addition, the broken liquid metal particles can be used for a bridging role in the metal filler/liquid metal particles/polymer composite. To circumvent the printing resolution encountered with the micron size liquid metal particles, the colloidal liquid metal particle suspension can be a solution for the submicron patterning. In this case, one of the parameters for controlling the liquid metal particle size is the concentration of chemical functionalization compound. However, since the higher concentration of chemical compounds on the shell inhibits the coalescence of the liquid metal particles, the tuning of the optimized concentration of chemical compounds is an important point for electrode applications. In addition, the smaller size of the liquid metal particles could result in a higher fraction of oxide layer formation on the liquid metal particles, which indicates that the parts of the insulating or semiconducting layer and the solid-state layer are increasing, resulting in the higher resistance. In order to obtain a micro-patterned electrode, the smaller size of the liquid metal particles is required, but the aforementioned issues remain.

On the other hand, in a dielectric application or thermally conductive materials, preserving the particle shape of the liquid metal without coalescence is necessary. Since the oxide layer on the liquid metal particles provides not only affinity with a silicone-based polymer, such as PDMS, but also the dielectric performance, sustaining the oxide layer on the liquid metal is an important factor for utilizing a dielectric application such as triboelectric energy harvester or capacitive sensor. In addition, the high thermal conductivity of the liquid metal (~26 W mK^{-1}) can be utilized as heat dissipation materials for a flexible device. Since the dielectric constant and thermal conductivity of the composite are strongly dependent on the amount of liquid metal particles, the preparation of a dielectric layer or thermally conductive layer with the higher amount and smaller size of liquid metal particles is required. To overcome the limits, the surface-initiated polymerization of liquid metal particles can be

an alternative to preparing dielectric and thermally conductive functional materials. The surface-initiated polymerization on the liquid metal particles makes the polymer encapsulate the liquid metal particles. The polymer matrix can then protect the liquid metal particles, and the high concentration of liquid metal particles in the polymer composite is possible.

For other applications, owing to the low standard reduction potential of Ga in the liquid metal (-0.560 V), another metal can be decorated on the surface of the liquid metal particles. For example, a galvanic replacement can be a useful method for the sub-micron electrode with the employment of liquid metal particles. Due to the difference of the standard reduction potential between Ga^{3+}/Ga and noble metal ion/noble metal, such as Au^{+}/Au, the noble metal can be decorated on the surface of the liquid metal, and an electrically conductive path can be provided by the percolation of the reduced noble metal without the coalescence of the liquid metal particles. Besides, the decoration of a metal or metal oxide on the liquid metal particles can be employed in soft robotics. In addition, due to the electrochemical activity of Ga and the high diffusivity of ions in the liquid metal, the liquid metal particles showed a promising potential for energy storage applications.

Owing to the non-toxic property, the Ga-based liquid metal can be utilized in biomedicine. In this case, the surface functionalization of liquid metal particles can be conducted with chemical compounds containing a drug for cure. In particular, since the functionalized liquid metal particles release the drug under the acidic condition, the tumor-target therapy is possible. In this case, the selection of the molecules, which can be functionalized on the surface of the liquid metal particles and can deliver the drug to the target point, should be considered. In addition, Ga and In (or Sn) were separated in an aqueous atmosphere when the Ga-based liquid metal was heated, and the Ga tends to convert into GaOOH, which has a crystalline nanorod structure. The drug that is functionalized on the liquid metal surface can be released by locally increasing the temperature. However, in this case, the effect of crystalized GaOOH in the organs or blood stream should be investigated, and the safety of that should be also confirmed.

This article focused on the strategies of the surface functionalization of the liquid metal particles for various applications. Owing to the liquid phase, low toxicity, high electrical, and thermal conductivity, the liquid metal and its composite have a potential for advanced soft electronics, robotics, or biomedicine. Depending on the application, the role of the liquid metal particles should be considered. Accordingly, the suitable surface modification of the liquid metal should be conducted. Even though several challenges still remain, the development of the surface modification of liquid metal can provide opportunities for the core materials of the next generation of flexible and deformable devices.

Conflicts of interest

There are no conflicts to declare.

Acknowledgements

References

1 C. Gong, J. Liang, W. Hu, X. Niu, S. Ma, H. T. Hahn and Q. Pei, *Adv. Mater.*, 2013, **25**, 4186–4191.

2 T. Sekitani, Y. Noguchi, K. Hata, T. Fukushima, T. Aida and T. Someya, *Science*, 2008, **321**, 1468–1472.

3 H.-B. Zhang, W.-G. Zheng, Q. Yan, Y. Yang, J.-W. Wang, Z.-H. Lu, G.-Y. Ji and Z.-Z. Yu, *Polymer*, 2010, **51**, 1191–1196.

4 A. M. Marconnet, N. Yamamoto, M. A. Panzer, B. L. Wardle and K. E. Goodson, *ACS Nano*, 2011, **5**, 4818–4825.

5 K. Uetani, T. Okada and H. T. Oyama, *J. Mater. Chem. C*, 2016, **4**, 9697–9703.

6 J. Wang, C. Yan, W. Kang and P. S. Lee, *Nanoscale*, 2014, **6**, 10734–10739.

7 T. Chen, H. Peng, M. Durstock and L. Dai, *Sci. Rep.*, 2014, **4**, 3612.

8 M. D. Dickey, *Adv. Mater.*, 2017, **29**, 1606425.

9 D. Zrnic and D. S. Swatik, *J. Less-Common Met.*, 1969, **18**, 67–68.

10 Q. Gao, H. Li, J. Zhang, Z. Xie, J. Zhang and L. Wang, *Sci. Rep.*, 2019, **9**, 5908.

11 M. R. Khan, C. Trlica and M. D. Dickey, *Adv. Funct. Mater.*, 2015, **25**, 671–678.

12 J.-H. So and M. D. Dickey, *Lab Chip*, 2011, **11**, 905–911.

13 M. R. Khan, C. B. Eaker, E. F. Bowden and M. D. Dickey, *Proc. Natl. Acad. Sci. U. S. A.*, 2014, **111**, 14047–14051.

14 S.-Y. Tang, R. Qiao, S. Yan, D. Yuan, Q. Zhao, G. Yun, T. P. Davis and W. Li, *Small*, 2018, **14**, 1800118.

15 C. J. Thrasher, Z. J. Farrell, N. J. Morris, C. L. Willey and C. E. Tabor, *Adv. Mater.*, 2019, **31**, 1903864.

16 Y. Lu, Q. Hu, Y. Lin, D. B. Pacardo, C. Wang, W. Sun, F. S. Ligler, M. D. Dickey and Z. Gu, *Nat. Commun.*, 2015, **6**, 10066.

17 O. Oloye, C. Tang, A. Du, G. Will and A. P. O'Mullane, *Nanoscale*, 2019, **11**, 9705–9715.

18 F. Hoshyargar, J. Crawford and A. P. O'Mullane, *J. Am. Chem. Soc.*, 2017, **139**, 1464–1471.

19 M. Karbalaei Akbari, Z. Hai, Z. Wei, R. K. Ramachandran, C. Detavernier, M. Patel, J. Kim, F. Verpoort, H. Lu and S. Zhuiykov, *J. Mater. Chem. C*, 2019, **7**, 5584–5595.

20 M. D. Dickey, *ACS Appl. Mater. Interfaces*, 2014, **6**, 18369–18379.

21 Y. Lin, J. Genzer and M. D. Dickey, *Adv. Sci.*, 2020, **n/a**, 2000192.

22 T. Hutter, W.-A. C. Bauer, S. R. Elliott and W. T. S. Huck, *Adv. Funct. Mater.*, 2012, **22**, 2624–2631.

23 J. Thelen, M. D. Dickey and T. Ward, *Lab Chip*, 2012, **12**, 3961–3967.

24 S. Park, G. Thangavel, K. Parida, S. Li and P. S. Lee, *Adv. Mater.*, 2019, **31**, 1805536.

25 J. Wang, G. Cai, S. Li, D. Gao, J. Xiong and P. S. Lee, *Adv. Mater.*, 2018, **30**, 1706157.

26 I. D. Tevis, L. B. Newcomb and M. Thuo, *Langmuir*, 2014, **30**, 14308–14313.

27 J. N. Hohman, M. Kim, G. A. Wadsworth, H. R. Bednar, J. Jiang, M. A. LeThai and P. S. Weiss, *Nano Lett.*, 2011, **11**, 5104–5110.

28 X. Li, M. Li, J. Xu, J. You, Z. Yang and C. Li, *Nat. Commun.*, 2019, **10**, 3514.

29 X. Li, M. Li, L. Zong, X. Wu, J. You, P. Du and C. Li, *Adv. Funct. Mater.*, 2018, **28**, 1804197.

30 J. Yan, M. H. Malakooti, Z. Lu, Z. Wang, N. Kazem, C. Pan, M. R. Bockstaller, C. Majidi and K. Matyjaszewski, *Nat. Nanotechnol.*, 2019, **14**, 684–690.

31 J. Yan, X. Pan, Z. Wang, Z. Lu, Y. Wang, L. Liu, J. Zhang, C. Ho, M. R. Bockstaller and K. Matyjaszewski, *Chem. Mater.*, 2017, **29**, 4963–4969.

32 M. A. White, J. A. Johnson, J. T. Koberstein and N. J. Turro, *J. Am. Chem. Soc.*, 2006, **128**, 11356–11357.

33 L. Tang, S. Cheng, L. Zhang, H. Mi, L. Mou, S. Yang, Z. Huang, X. Shi and X. Jiang, *iScience*, 2018, **4**, 302–311.

34 M. J. Ford, C. P. Ambulo, T. A. Kent, E. J. Markvicka, C. Pan, J. Malen, T. H. Ware and C. Majidi, *Proc. Natl. Acad. Sci. U. S. A.*, 2019, **116**, 21438–21444.

35 J. W. Boley, E. L. White and R. K. Kramer, *Adv. Mater.*, 2015, **27**, 2355–2360.

36 E. J. Markvicka, M. D. Bartlett, X. Huang and C. Majidi, *Nat. Mater.*, 2018, **17**, 618–624.

37 J.-H. Fu, J.-Y. Gao, S. Chen, P. Qin, J.-T. Shi and J. Liu, *RSC Adv.*, 2019, **9**, 35102–35108.

38 R. Tutika, S. Kmiec, A. B. M. T. Haque, S. W. Martin and M. D. Bartlett, *ACS Appl. Mater. Interfaces*, 2019, **11**, 17873–17883.

39 M. D. Bartlett, N. Kazem, M. J. Powell-Palm, X. Huang, W. Sun, J. A. Malen and C. Majidi, *Proc. Natl. Acad. Sci. U. S. A.*, 2017, **114**, 2143–2148.

40 L. Sheng, J. Zhang and J. Liu, *Adv. Mater.*, 2014, **26**, 6036–6042.

41 X. Tang, S.-Y. Tang, V. Sivan, W. Zhang, A. Mitchell, K. Kalantar-zadeh and K. Khoshmanesh, *Appl. Phys. Lett.*, 2013, **103**, 174104.

42 W. Gao, A. Pei and J. Wang, *ACS Nano*, 2012, **6**, 8432–8438.

43 R. Guo, X. Sun, B. Yuan, H. Wang and J. Liu, *Adv. Sci.*, 2019, **6**, 1901478.

44 J. Jeon, J.-B. Lee, S. K. Chung and D. Kim, *Lab Chip*, 2017, **17**, 128–133.

45 J. Jeon, J. Lee, S. K. Chung and D. Kim, 2015.

46 J. Jeon, J. Lee, S. K. Chung and D. Kim, *J. Microelectromech. Syst.*, 2016, **25**, 1050–1057.

47 V. Sivan, S.-Y. Tang, A. P. O'Mullane, P. Petersen, N. Eshtiaghi, K. Kalantar-zadeh and A. Mitchell, *Adv. Funct. Mater.*, 2013, **23**, 144–152.

48 L. C. Cadwallader, *Gallium Safety in the Laboratory*, United States, 2003.

49 Y. Yu and E. Miyako, *Angew. Chem., Int. Ed.*, 2017, **56**, 13606–13611.

50 L. J. Norrby, *J. Chem. Educ.*, 1991, **68**, 110.

51 R. H. Müller and J. F. Petras, *J. Am. Chem. Soc.*, 1938, **60**, 2990–2993.

52 S. A. Moros, *Anal. Chem.*, 1962, **34**, 1584–1587.

53 A. Spencer, *Aust. Dent. J.*, 2000, **45**, 224–234.

54 R. W. Powell and E. C. Bullard, *Proc. R. Soc. London, Ser. A*, 1951, **209**, 525–541.

55 T. Daeneke, K. Khoshmanesh, N. Mahmood, I. A. de Castro, D. Esrafilzadeh, S. J. Barrow, M. D. Dickey and K. Kalantar-zadeh, *Chem. Soc. Rev.*, 2018, **47**, 4073–4111.

56 T. J. Anderson and I. Ansara, *J. Phase Equilib.*, 1991, **12**, 64–72.

57 T. J. Anderson and I. Ansara, *J. Phase Equilib.*, 1992, **13**, 181–189.

58 G. N. van Ingen, J. Kapteijn and J. L. Meijering, *Scr. Metall.*, 1970, **4**, 733–736.

59 S. Yu and M. Kaviany, *J. Chem. Phys.*, 2014, **140**, 064303.

60 Y. Lin, C. Cooper, M. Wang, J. J. Adams, J. Genzer and M. D. Dickey, *Small*, 2015, **11**, 6397–6403.

61 M. J. Regan, H. Tostmann, P. S. Pershan, O. M. Magnussen, E. DiMasi, B. M. Ocko and M. Deutsch, *Phys. Rev. B*, 1997, **55**, 10786–10790.

62 K. Doudrick, S. Liu, E. M. Mutunga, K. L. Klein, V. Damle, K. K. Varanasi and K. Rykaczewski, *Langmuir*, 2014, **30**, 6867–6877.

63 C. B. Eaker and M. D. Dickey, *Appl. Phys. Rev.*, 2016, **3**, 031103.

64 C. Pan, E. J. Markvicka, M. H. Malakooti, J. Yan, L. Hu, K. Matyjaszewski and C. Majidi, *Adv. Mater.*, 2019, **31**, 1900663.

65 Y. Lin, Y. Liu, J. Genzer and M. D. Dickey, *Chem. Sci.*, 2017, **8**, 3832–3837.

66 Z. J. Farrell and C. Tabor, *Langmuir*, 2018, **34**, 234–240.

67 S. A. Chechetka, Y. Yu, X. Zhen, M. Pramanik, K. Pu and E. Miyako, *Nat. Commun.*, 2017, **8**, 15432.

68 L. Ren, J. Zhuang, G. Casillas, H. Feng, Y. Liu, X. Xu, Y. Liu, J. Chen, Y. Du, L. Jiang and S. X. Dou, *Adv. Funct. Mater.*, 2016, **26**, 8111–8118.

69 S.-Y. Tang, R. Qiao, Y. Lin, Y. Li, Q. Zhao, D. Yuan, G. Yun, J. Guo, M. D. Dickey, T. J. Huang, T. P. Davis, K. Kalantar-Zadeh and W. Li, *Adv. Mater. Technol.*, 2019, **4**, 1800420.

70 D. I. Kreller, G. Gibson, W. Novak, G. W. Van Loon and J. H. Horton, *Colloids Surf., A*, 2003, **212**, 249–264.

71 P. H. Mutin, G. Guerrero and A. Vioux, *J. Mater. Chem.*, 2005, **15**, 3761–3768.

72 N. Wu, L. Fu, M. Su, M. Aslam, K. C. Wong and V. P. Dravid, *Nano Lett.*, 2004, **4**, 383–386.

73 L. Zhang, R. He and H.-C. Gu, *Appl. Surf. Sci.*, 2006, **253**, 2611–2617.

74 Z. J. Farrell, N. Reger, I. Anderson, E. Gawalt and C. Tabor, *J. Phys. Chem. C*, 2018, **122**, 26393–26400.

75 C. Zhang, F.-M. Allioux, M. A. Rahim, J. Han, J. Tang, M. B. Ghasemian, S.-Y. Tang, M. Mayyas, T. Daeneke, P. Le-Clech, R. B. Kaner, D. Esrafilzadeh and K. Kalantar-Zadeh, *Chem. Mater.*, 2020, **32**, 4808–4819.

76 T. Gan, W. Shang, S. Handschuh-Wang and X. Zhou, *Small*, 2019, **15**, 1804838.

77 Y. Liu, Q. Wang, J. Deng and W. Zhang, *Chem. Commun.*, 2020, **56**, 1851–1854.

78 A. Bard, *Standard Potentials in Aqueous Solution*, CRC Press, New York, 1985.

79 R. David and N. Miki, *Nanoscale*, 2019, **11**, 21419–21432.

80 D. L. M. Desmaële, F. Rizzi, A. Qualtieri and M. De Vittorio, *J. Low Power Electron. Appl.*, 2018, **8**, 45.

81 B. Lertanantawong, P. Lertsathitphong and A. P. O'Mullane, *Electrochem. Commun.*, 2018, **93**, 15–19.

82 G. Yun, S.-Y. Tang, S. Sun, D. Yuan, Q. Zhao, L. Deng, S. Yan, H. Du, M. D. Dickey and W. Li, *Nat. Commun.*, 2019, **10**, 1300.

83 Y. R. Jeong, J. Kim, Z. Xie, Y. Xue, S. M. Won, G. Lee, S. W. Jin, S. Y. Hong, X. Feng, Y. Huang, J. A. Rogers and J. S. Ha, *NPG Asia Mater.*, 2017, **9**, e443.

84 D. C. Edwards, *J. Mater. Sci.*, 1990, **25**, 4175–4185.

85 R. Avolio, G. Gentile, M. Avella, C. Carfagna and M. E. Errico, *Eur. Polym. J.*, 2013, **49**, 419–427.

86 N. Kazem, M. D. Bartlett and C. Majidi, *Adv. Mater.*, 2018, **30**, 1706594.

87 Y. Chung and C.-W. Lee, *J. Electrochem. Sci. Technol.*, 2013, **4**, 1–18.

88 H. Wang, B. Yuan, S. Liang, R. Guo, W. Rao, X. Wang, H. Chang, Y. Ding, J. Liu and L. Wang, *Mater. Horiz.*, 2018, **5**, 222–229.

89 G. Liu, J. Y. Kim, M. Wang, J.-Y. Woo, L. Wang, D. Zou and J. K. Lee, *Adv. Energy Mater.*, 2018, **8**, 1703652.

90 J. N. Butler and M. L. Meehan, *Trans. Faraday Soc.*, 1966, **62**, 3524–3534.

91 M. Higashiwaki, K. Sasaki, A. Kuramata, T. Masui and S. Yamakoshi, *Appl. Phys. Lett.*, 2012, **100**, 013504.

92 B. J. Blaiszik, S. L. B. Kramer, M. E. Grady, D. A. McIlroy, J. S. Moore, N. R. Sottos and S. R. White, *Adv. Mater.*, 2012, **24**, 398–401.

93 J.-E. Park, H. S. Kang, J. Baek, T. H. Park, S. Oh, H. Lee, M. Koo and C. Park, *ACS Nano*, 2019, **13**, 9122–9130.

94 A. Fassler and C. Majidi, *Adv. Mater.*, 2015, **27**, 1928–1932.

95 X. Wang, R. Guo and J. Liu, *Adv. Mater. Technol.*, 2019, **4**, 1800549.

96 X. Guo, L. Zhang, Y. Ding, J. B. Goodenough and G. Yu, *Energy Environ. Sci.*, 2019, **12**, 2605–2619.

97 R. D. Deshpande, J. Li, Y.-T. Cheng and M. W. Verbrugge, *J. Electrochem. Soc.*, 2011, **158**, A845.

98 S. N. S. Hapuarachchi, K. C. Wasalathilake, D. P. Siriwardena, J. Y. Nerkar, H. Chen, S. Zhang, Y. Liu, J.-c. Zheng, D. V. Golberg, A. P. O'Mullane and C. Yan, *ACS Appl. Energy Mater.*, 2020, **3**, 5147–5152.

99 D. K. Sarfo, R. R. Taylor and A. P. O'Mullane, *ACS Appl. Electron. Mater.*, 2020, **2**, 2921–2928.

100 X. Guo, Y. Ding, L. Xue, L. Zhang, C. Zhang, J. B. Goodenough and G. Yu, *Adv. Funct. Mater.*, 2018, **28**, 1804649.

101 S. Nayak, Y. Li, W. Tay, E. Zamburg, D. Singh, C. Lee, S. J. A. Koh, P. Chia and A. V.-Y. Thean, *Nano Energy*, 2019, **64**, 103912.

102 S. Gao, R. Wang, C. Ma, Z. Chen, Y. Wang, M. Wu, Z. Tang, N. Bao, D. Ding, W. Wu, F. Fan and W. Wu, *J. Mater. Chem. A*, 2019, **7**, 7109–7117.

103 Q. Ye, Y. Wu, Y. Qi, L. Shi, S. Huang, L. Zhang, M. Li, W. Li, X. Zeng, H. Wo, X. Wang, S. Dong, S. Ramakrishna and J. Luo, *Nano Energy*, 2019, **61**, 381–388.

104 K. Parida, G. Thangavel, G. Cai, X. Zhou, S. Park, J. Xiong and P. S. Lee, *Nat. Commun.*, 2019, **10**, 2158.

105 S. H. Jeong, S. Chen, J. Huo, E. K. Gamstedt, J. Liu, S.-L. Zhang, Z.-B. Zhang, K. Hjort and Z. Wu, *Sci. Rep.*, 2015, **5**, 18257.

106 M. I. Ralphs, N. Kemme, P. B. Vartak, E. Joseph, S. Tipnis, S. Turnage, K. N. Solanki, R. Y. Wang and K. Rykaczewski, *ACS Appl. Mater. Interfaces*, 2018, **10**, 2083–2092.

107 Y. Sargolzaeiaval, V. P. Ramesh, T. V. Neumann, R. Miles, M. D. Dickey and M. C. Öztürk, *ECS J. Solid State Sci. Technol.*, 2019, **8**, P357–P362.

108 M. H. Malakooti, N. Kazem, J. Yan, C. Pan, E. J. Markvicka, K. Matyjaszewski and C. Majidi, *Adv. Funct. Mater.*, 2019, **29**, 1906098.

109 M. Zadan, M. H. Malakooti and C. Majidi, *ACS Appl. Mater. Interfaces*, 2020, **12**, 17921–17928.

110 E. G. Bakhoum and M. H. M. Cheng, *IEEE Trans. Compon. Packag. Technol.*, 2010, **33**, 79–83.

111 D.-J. Won, S. Baek, H. Kim and J. Kim, *Sens. Actuators, A*, 2015, **235**, 151–157.

112 C. B. Cooper, K. Arutselvan, Y. Liu, D. Armstrong, Y. Lin, M. R. Khan, J. Genzer and M. D. Dickey, *Adv. Funct. Mater.*, 2017, **27**, 1605630.

113 Y. Lu, Y. Lin, Z. Chen, Q. Hu, Y. Liu, S. Yu, W. Gao, M. D. Dickey and Z. Gu, *Nano Lett.*, 2017, **17**, 2138–2145.

114 N. B. Morley, J. Burris, L. C. Cadwallader and M. D. Nornberg, *Rev. Sci. Instrum.*, 2008, **79**, 056107.

115 S. Cheng and Z. Wu, *Lab Chip*, 2012, **12**, 2782–2791.

116 M. D. Dickey, R. C. Chiechi, R. J. Larsen, E. A. Weiss, D. A. Weitz and G. M. Whitesides, *Adv. Funct. Mater.*, 2008, **18**, 1097–1104.